# 3′-Phosphoadenosine 5′-Phosphosulfate Allosterically Regulates Sulfotransferase Turnover

Ting Wang, Ian Cook, and Thomas S. Leyh*

Department of Microbiology and Immunology, Albert Einstein College of Medicine, 1300 Morris Park Avenue, Bronx, New York 10461-1926, United States

S *Supporting Information*

ABSTRACT: Human cytosolic sulfotransferases (SULTs) regulate the activities of thousands of small molecules—metabolites, drugs, and other xenobiotics—via the transfer of the sulfuryl moiety (-SO$_3$) from 3′-phosphoadenosine 5′-phosphosulfate (PAPS) to the hydroxyls and primary amines of acceptors. SULT1A1 is the most abundant SULT in liver and has the broadest substrate spectrum of any SULT. Here we present the discovery of a new form of SULT1A1 allosteric regulation that modulates the catalytic efficiency of the enzyme over a 130-fold dynamic range. The molecular basis of the regulation is explored

in detail and is shown to be rooted in an energetic coupling between the active-site caps of adjacent subunits in the SULT1A1 dimer. The first nucleotide to bind causes closure of the cap to which it is bound and at the same time stabilizes the cap in the adjacent subunit in the open position. Binding of the second nucleotide causes both caps to open. Cap closure sterically controls active-site access of the nucleotide and acceptor; consequently, the structural changes in the cap that occur as a function of nucleotide occupancy lead to changes in the substrate affinities and turnover of the enzyme. PAPS levels in tissues from a variety of organs suggest that the catalytic efficiency of the enzyme varies across tissues over the full 130-fold range and that efficiency is greatest in those tissues that experience the greatest xenobiotic "load".
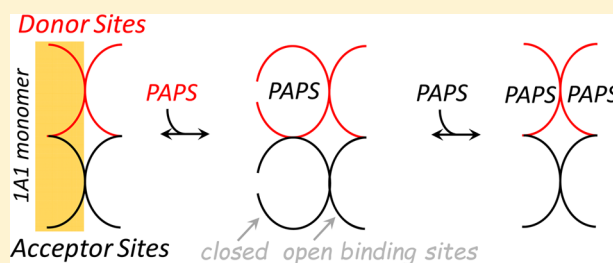
Transfer of the sulfuryl group (-SO$_3$) to and from small-molecule metabolites switches these compounds between distinctly different functional states. Sulfonation of the agonists and antagonists that bind nuclear and dopamine receptors, which regulate scores of complex cellular functions, typically decreases but can also enhance their affinities for their targets by orders of magnitude. The inability to maintain the requisite balance of sulfonated and nonsulfonated forms of a particular compound(s) has been linked to human diseases, including breast[1] and endometrium[2] cancer, Parkinson's disease,[3] cystic fibrosis,[4] and hemophilia.[5]

Small-molecule sulfonation is catalyzed by a small, approximately 13-member,[6] family of enzymes, the cytosolic sulfotransferases (SULTs). The donor in these reactions is the nucleotide PAPS (3′-phosphoadenosine 5′-phosphosulfate), also known as activated sulfate. The remarkably high chemical potential of the phosphoric–sulfuric acid anhydride bond in PAPS potentiates the sulfuryl moiety for energetically favorable transfer to recipients.[7] The acceptors are the hydroxyls and primary amines of hundreds, if not thousands, of small molecules—endogenous metabolites, drugs, and other xenobiotics.[8] In addition to their roles in regulating endogenous metabolites, SULTs provide a critical defensive function; they detoxify compounds, particularly xenobiotics, by preventing them from binding adventitiously to receptors and target them for degradation and elimination.[1,9,10]

SULT1A1, the focus of this study, is the predominant SULT isoform in liver and is responsible for the majority of the sulfonation that occurs there.[11] Consistent with its role in detoxifying xenobiotics—an enormous, complex category of compounds—the substrate spectrum of SULT1A1 is the broadest of any SULT.[6] Recent studies of the molecular basis of SULT substrate specificity reveal that SULTs extensively utilize a conserved, dynamic 30-residue active-site "cap" in selecting their substrates. In the unliganded state, the cap is open.[12−14] As PAPS binds, the cap closes and molecular "pores" that sterically restrict ligand access are formed at the acceptor and donor sites. PAPS is too large to pass through the nucleotide pore, and its entry and departure require that the cap open.[13] Certain acceptors are small enough to pass unrestricted through the acceptor pore; others are not, and their binding, like that of PAPS, also requires cap opening.[15] Here we show that opening and closing of the caps in the SULT1A1 dimer are allosterically coordinated by the binding of nucleotide. Binding of the first and second nucleotides produces different cap configurations, and the catalytic efficiencies of these forms differ over a 130-fold dynamic range. For the first time, it is clear that a nucleotide can function as an allostere in SULT systems.

■ MATERIALS AND METHODS

The experimental materials and their sources are as follows. Adenosine monophosphate (AMP), dithiothreitol (DTT), dimethyl sulfoxide (DMSO), ethylenediaminetetraacetic acid (EDTA), 1-hydroxypyrene (1-HP), 4-hydroxytamoxifen (afimoxifene, TAM), imidazole, isopropyl thio-β-D-galactopyranoside (IPTG), Luria broth (LB), lysozyme, β-mercaptoethanol (β-ME), pepstatin A, Na_2HPO_4, and NaH_2PO_4 were obtained from Sigma. Ampicillin, HEPES, KCl, KOH, $MgCl_2$, NaCl, and phenylmethanesulfonyl fluoride (PMSF) were purchased from Fisher Scientific. Glutathione- and nickel-chelating resins were obtained from GE Healthcare. Competent *Escherichia coli* [BL21(DE3)] cells were purchased from Agilent Technologies. PAP, PAPS, and [^{35}S]PAPS were synthesized in house as previously described[12,16,17] and were ≥98% pure as assessed by anion-exchange high-performance liquid chromatography.

Protein Purification. The open reading frame of the human SULT1A1 DNA was codon-optimized for *E. coli* (MR. GENE) and inserted into a pGEX6 vector containing a His/GST/MBP triple affinity tag.[14] The enzyme was expressed in *E. coli* BL21(DE3) and purified according to a published protocol.[17] Briefly, enzyme expression was induced with IPTG (0.50 mM) in LB medium at 16 °C for 14 h. The cells were pelleted, resuspended in lysis buffer, sonicated, and centrifuged. The supernatant was loaded onto a Chelating Sepharose Fast Flow column charged with Ni^{2+}. The enzyme was eluted with imidazole (10 mM) onto a Glutathione Sepharose column and then eluted with glutathione (10 mM). The tag was cleaved from the enzyme by precision protease, and the enzyme was separated from the tag using a glutathione resin. Finally, the protein was concentrated using a Millipore Ultrafiltration Disc (Ultracel 10 kDa cutoff), and the concentration was determined spectrophotometrically (ε_{280} = 54 mM^{-1} cm^{-1}).[14] The enzyme was flash-frozen and stored at −80 °C.

Equilibrium Binding of PAPS to SULT1A1. Binding of PAPS to SULT1A1 was monitored via ligand-dependent changes in intrinsic fluorescence (λ_{ex} = 290 nm; λ_{em} = 345 nm). Typically, PAPS was titrated into solutions containing SULT1A1, $MgCl_2$ (5.0 mM), and NaPO$_4$ (50 mM) at pH 7.2 and 25 ± 2 °C. The PAPS concentrations used in the titration depicted in Figure 1D were high enough to cause inner-filter effects. Consequently, λ_{ex} was shifted to 297 nm to lower the PAPS absorbance (ε_{297} = 0.43 mM^{-1} cm^{-1}). Despite the lowered absorbance, inner-filter effects were detected at ≥60 μM PAPS. To correct for these effects, control titrations in which AMP (which does not bind SULT1A1) was substituted for PAPS were performed and the PAPS titration data were corrected accordingly. All titrations were performed in triplicate, and the averaged data were least-squares fit using a model that assumes a single binding site per dimer.[12]

Pre-Steady-State PAPS Binding Studies. Pre-steady-state binding experiments were performed using an Applied Photophysics SX20 stopped-flow spectrofluorimeter. SULT1A1 fluorescence was excited at 290 nm and detected above 330 nm using a cutoff filter. k_{on} and k_{off} for binding to the high-affinity site were obtained by rapidly mixing [1:1 (v:v)] a solution containing SULT1A1 (30 nM, dimer), $MgCl_2$ (5.0 mM), and NaPO$_4$ (25 mM) at pH 7.2 and 25 ± 2 °C with a solution that was identical except that it contained PAPS and was without enzyme. k_{on} and k_{off} for the binding to the low-affinity site were determined by pre-equilibrating the dimer (2.0 μM) with PAPS

(4.0 μM) and then rapidly mixing the equilibrated solution [1:1 (v:v)] with a solution that was identical except for the PAPS concentrations and the fact that it lacked enzyme. The reactions were pseudo-first-order with respect to PAPS concentration. Three independently determined progress curves (each an average of 8−10 binding reactions) were collected at four separate PAPS concentrations. The apparent rate constant (k_{obs}) at a given PAPS concentration was obtained by fitting the average of the three curves to a single-exponential equation. k_{on} and k_{off} were obtained from the slopes and intercepts, respectively, predicted by linear least-squares analysis of four-point k_{obs} versus PAPS concentration plots.[18]

Equilibrium Binding of TAM and 1-HP to SULT1A1. Binding of an acceptor to three different enzyme forms [E, E·PAP, and E·(PAP)$_2$] was monitored via ligand-induced changes in the intrinsic fluorescence of the enzyme (λ_{ex} = 290 nm; λ_{em} = 345 nm). Acceptors were titrated into a solution containing SULT1A1 (0.05−10 μM, dimer), PAP (0−500 μM), $MgCl_2$ (5.0 mM), and NaPO$_4$ (25 mM) at pH 7.2 and 25 ± 2 °C. Titrations were performed in triplicate. Data were averaged and least-squares fit using a model that assumes a single binding site per monomer.[12,17]

Activation of SULT1A1. The initial rate response of SULT1A1 to nucleotide binding at the high- and low-affinity sites was studied using 1-HP, a fluorescent acceptor. 1-HP and its sulfonated counterpart (1-HPS) fluoresce at a λ_{ex} of 320 nm, but the intensity ratio at a λ_{em} of 380 nm is >100 in favor of 1-HPS. Reaction progress was monitored via 1-HPS fluorescence (λ_{ex} = 320 nm; λ_{em} = 380 nm). Reactions were initiated by addition of PAPS, and the conditions were as follows: SULT1A1 (1.0 nM, dimer), 1-HP (160 μM, 20K_d), $MgCl_2$ (5.0 mM), NaPO$_4$ (50 mM), pH 7.2, and 25 ± 2.0 °C. The PAPS concentration was the limiting substrate in all cases, and it was ≤5% consumed at the end point of the reactions. The experiments were performed in duplicate. The K_m and k_{cat} of 1-HP for the doubly occupied enzyme were determined using a saturating PAPS concentration (2.0 μM), and a range of 1-HP concentrations (8.0−200 nM, 0.2−5K_m). The kinetic constants for 1-HP sulfation with the singly occupied enzyme were obtained using the same strategy except that the PAPS concentration was sufficient to saturate only the first site (0.30 μM). Initial rate constants were obtained using a weighted least-squares fit of the data in double-reciprocal format.[19]

Initial Rate Kinetics of TAM Sulfation. The initial rate of TAM sulfation was measured using radiolabeled [^{35}S]PAPS. Reaction conditions included SULT1A1 (10 nM, dimer), [^{35}S]PAPS (3.0 or 250 μM, 14 nCi/reaction), TAM (0.12−70 μM, 0.20−5.0K_m), $MgCl_2$ (5.0 mM), NaPO$_4$ (50 mM), pH 7.2, and 25 ± 2 °C. The reactions were initiated by the addition of PAPS to a final volume of 10 μL. The reactions were quenched after 10−50 min with 1.0 μL of 0.10 M NaOH and then the mixtures neutralized with HCl. Samples were then boiled for 1.0 min and centrifuged for 5.0 min at 12100g. The samples were spotted onto a reverse phase thin layer chromatography plate and separated using a running buffer containing methylene chloride, methanol, water, and ammonium hydroxide (90:16:3.5:0.50 volume ratio). Radiolabeled products were visualized and quantitated using a STORM imaging system.

■ RESULTS AND DISCUSSION

Biphasic Binding of PAPS to SULT1A1. The fluorescence titrations depicted in Figure 1A−D present what appears to be
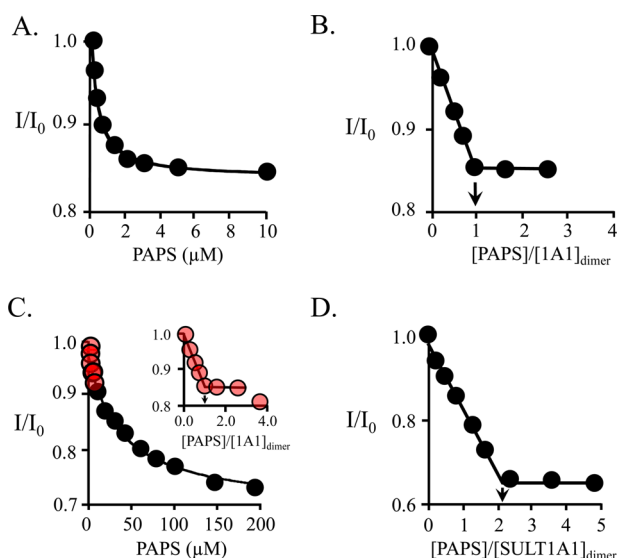
Figure 1. Equilibrium binding of PAPS to SULT1A1. (A) PAPS binding to the high-affinity subunit. Binding was monitored via ligand-induced changes in the intrinsic fluorescence of SULT1A1 (λ_{ex} = 295 nm; λ_{em} = 345 nm). Reaction conditions included SULT1A1 (0.05 μM, dimer), $MgCl_2$ (5.0 mM), $NaPO_4$ (50 mM), pH 7.2, and 25 ± 2 °C. Each point is the average of three independent determinations. The solid line through the data represents a least-squares fit using a model that assumes a single binding site per dimer. K_d = 0.37 ± 0.05 μM. (B) PAPS binding stoichiometry at the high-affinity site. The conditions were identical to those in described for panel A except that [SULT1A1] = 3.0 μM dimer ($16K_d$). The stoichiometry was 1.1 ± 0.2 PAPS molecules per dimer. (C) PAPS binding at the low-affinity site. Experimental conditions were identical to those in described for panel B. PAPS binding is biphasic. The high- and low-affinity phases are colored red (inset) and black, respectively. The line through the points represents a least-squares fit to the low-affinity phase using a model that assumes a single binding site per dimer. K_d = 30 ± 4 μM. (D) Full-site PAPS binding stoichiometry. The reaction conditions were identical to those described for panel A except that [SULT1A1] = 475 μM dimer ($16K_d$ for the low-affinity site). The stoichiometry was 2.1 ± 0.2 PAPS molecules per dimer, or 1.1 ± 0.1 per subunit.

the first example of the biphasic binding of PAPS to SULT1A1, or any SULT. The conditions of the titration pairs, A/B and C/D, were selected to yield affinities and stoichiometries, respectively, of PAPS binding to the high-affinity (A/B) and low-affinity (C/D) sites of the enzyme. The enzyme active-site concentrations used in the "affinity-constant" titrations (A and C) were set below (≤0.14) K_d, while those used in "stoichiometry" titrations (B and D) were ≥15K_d.

The affinity of PAPS for the high-affinity site of SULT1A1 [K_d = 0.37 ± 0.05 μM (Table 1)] is virtually identical to that for other SULTs;[12,14,16] its stoichiometry, however, is not.[12,17] A second titration, at [SULT1A1] = 16K_d, reveals that the stoichiometry of PAPS binding at the high-affinity site is 1.1 ± 0.1 per SULT1A1 dimer (Figure 1B). Clearly, only one subunit in each dimer exhibits high affinity. This finding stands in

Table 1. PAPS Binding to SULT1A1

binding site	k_{on} ($\mu M^{-1} s^{-1}$)[a]	k_{off} (s^{-1})[a]	k_{off}/k_{on} (μM)[a]	K_d (μM)[a]
high-affinity	2.0 (0.1)	0.70 (0.05)	0.37 (0.04)	0.37 (0.05)
low-affinity	0.96 (0.01)	29 (1)	30 (3)	30 (4)

[a]Values in parentheses indicate one standard deviation.

contrast to the behaviors of SULT2A1 and SULT1E1, which bind 1 equiv of PAPS with high affinity at each dimer subunit.[14,16]

As the nucleotide concentration increases beyond saturation of the first site, a second binding phase is observed (Figure 1C). Red dots indicate the region of the titration in which binding occurs nearly exclusively at the high-affinity site, and as the inset shows, that site is loaded stoichiometrically. In the black-dotted region, a low-affinity site becomes saturated. The K_d associated with this region is 31 ± 4 μM. To confirm that this phase is associated with a single nucleotide site, its PAPS binding stoichiometry was determined (Figure 1D). The low-affinity site clearly binds one nucleotide, and thus, SULT1A1, like its siblings, binds one nucleotide at each subunit.

Most members of the SULT family harbor a conserved 30-residue active-site cap that covers both the nucleotide and acceptor binding pockets.[13,14,20] The nucleotide is nearly completely encapsulated when the cap is closed, and its addition and escape require that the cap open.[20] The cap of the ligand-free enzyme is predominantly open (≥95%[14,20]), while that of nucleotide-bound SULT1A1 is closed ~95% of the time.[14,20] As the cap closes at the acceptor site, a pore forms, creating an entrance to the acceptor binding pocket. The binding of acceptors small enough to pass through the pore is not affected by cap closure; nucleotide binding has no discernible effect on the k_{on} and k_{off} of such compounds. As acceptors become too large to pass through the pore, nucleotide binding causes their affinities to decrease by a factor given by the cap closure isomerization equilibrium constant (K_{iso}), which equals 26 for SULT1A1.[14] This decrease in affinity is due solely to a decrease in k_{on} and is caused by the nucleotide-induced 26-fold decrease in the concentration of the enzyme form to which large compounds can bind.

The Hypothesis. Given the coupling between PAPS binding and cap closure, and structural data indicating that the cap must open for PAPS to enter and depart, we reasoned that the decreased affinity for the second nucleotide could be due to reciprocal interactions between the open and closed forms of adjacent caps. If PAPS binding and closure at the first subunit stabilize the adjacent cap in either the open or closed position, the affinity of PAPS for the second site will decrease relative to that for the first. If closure is stabilized, k_{on} for PAPS binding will decrease, because closure decreases the concentration of the only form to which PAPS can bind, the cap-open form. If, on the other hand, the adjacent cap is stabilized in the open position, the k_{on} for binding to the tight and weak sites will be identical, because the caps of both the unliganded and singly liganded enzymes are fully open (≥95%). Thus, the change in affinity will be due solely to an increase in k_{off} that occurs because the nucleotide need not "wait" until the cap opens to depart.

The Test. To test the coupled cap model and distinguish between the adjacent cap open and closed mechanisms, the on and off rate constants for binding of PAPS to SULT1A1 were determined over a range of PAPS concentrations that probe binding to the tight and weak sites. PAPS binding was monitored via binding-induced changes in the intrinsic fluorescence of SULT1A1 (Figure S1 of the Supporting Information shows a typical PAPS binding reaction). The reactions were pseudo-first-order in PAPS concentration, and k_{obs} values were obtained by fitting progress curves to a single-exponential model. The results are compiled in the k_{obs} versus PAPS concentration plot presented in Figure 2A, which shows

two distinct linear phases indicative of two experimentally separable binding sites.
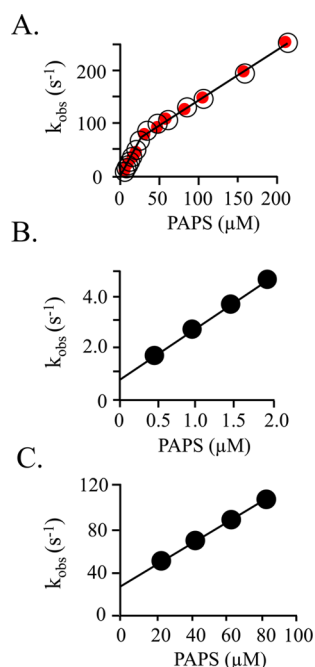

Figure 2. Pre-steady-state binding of PAPS to SULT1A1. (A) Composite k_{obs} vs [PAPS] plot. Two well-isolated binding phases are observed. Binding was monitored via changes in SULT1A1 intrinsic fluorescence (λ_{ex} = 290 nm; $\lambda_{em} \geq$ 330 nm). k_{obs} values are the average of three independent determinations. Reaction conditions included SULT1A1 (0.050 μM, dimer), MgCl$_2$ (5.0 mM), NaPO$_4$ (50 mM), pH 7.2, and 25 $\pm$ 2 °C. Red dots indicate the k_{obs} values predicted using the k_{on} and k_{off} values obtained from the experiments associated with panels B and C. (B) k_{obs} vs [PAPS] for the high-affinity subunit. Reaction conditions were identical to those described for panel A except that [SULT1A1] = 0.030 μM (dimer). k_{on} = 2.0 $\pm$ 0.2 μM^{-1} s^{-1}; k_{off} = 0.70 $\pm$ 0.02 s^{-1}. (C) k_{obs} vs [PAPS] for the low-affinity subunit. Reaction conditions were identical to those described for panel A except the SULT1A1 (2.0 μM, dimer) was equilibrated with PAPS [8.0 μM, 26$K_{d(high\ affinity)}$, 0.27$K_{d(low\ affinity)}$] before being mixed with PAPS at higher concentrations (20−80 μM). k_{on} = 0.96 $\pm$ 0.01 μM s^{-1}; k_{off} = 29 $\pm$ 1 s^{-1}. All reactions were pseudo-first-order in PAPS concentration.

The 81-fold difference in the affinities of the two PAPS binding sites allows them to be studied in isolation. At the PAPS concentrations used to construct the k_{obs} versus PAPS concentration plot in Figure 2B, the percentage of dimers with two molecules of PAPS bound at equilibrium ranges from 1.5 to 6.3%; hence, the signal from the doubly liganded species is negligible, and k_{on} and k_{off} for the high-affinity site can be obtained from a linear fit of the data. The rate constants associated with binding at the low-affinity site can be obtained using a pre-equilibration strategy. At 8.0 μM PAPS, the equilibrium distribution of enzyme forms is as follows: E, 2.5%; E·PAPS, 76%; E·(PAPS)$_2$, 21%. When this pre-equilibrated solution is mixed with PAPS at concentrations sufficiently high to saturate the second site, one observes conversion of the singly to doubly liganded species with a negligible contribution from other species. The result of such an experiment is shown in Figure 2C, and here again, k_{on} and k_{off} are obtained from the slope and intercept,[18] respectively. The accuracy of the four rate constants (k_{on} and k_{off} for high- and low-affinity binding) was

tested by using them to predict the k_{obs} values associated with Figure 2A. The predicted values are represented by red dots and closely match the experimental constants.

The Results. The rate constants associated with binding at the high- and low-affinity sites are compiled in Table 1. As the data indicate, the K_d values predicted by these constants are indistinguishable from those obtained from equilibrium binding studies. The off-rate constants reveal that nucleotide escapes from the low-affinity site 41-fold faster than from the high-affinity site. If the cap at the low-affinity site is "held" fully open ($\geq$95%) by binding at the tight site, and the escaping tendency of the nucleotide from the cap-open form of the high- and low-affinity sites is the same, the k_{on} values for binding at the first and second sites will be identical, because the cap in the subunit to which the nucleotide binds is open in both the unliganded and singly liganded enzyme forms. Thus, any fold difference in K_d will be due solely to differences in k_{off}. The results indicate that the changes in K_d (81-fold) and k_{off} (41-fold) differ by a factor of nearly 2 (i.e., 1.93). Within error, this same factor is given by the ratio of the k_{on} values for the low- and high-affinity sites, 2.08. A factor of 2 is readily explained if both subunits of the dimer are capable of binding the first ligand and only one can bind the second. In this scenario, k_{on} for the first site will appear to be 2-fold higher than that for the second because the probability of binding to the first site is twice that of the second, not because k_{on} values for binding to the subunits differ. If, as it appears, this is the case, the aggregate k_{on} for binding to the first site, 2.0 μM^{-1} s^{-1}, should be halved, to 1.0 μM^{-1} s^{-1}, and thus the k_{on} values for binding to the first and second sites are identical. In summary, the system behaves precisely as predicted by the adjacent cap open mechanism.

Linking to Acceptor-Site Binding. To define how cap behavior is coordinated at the four binding pockets of the enzyme, the PAPS dependence of the open or closed status of the acceptor binding sites was probed using a large acceptor [4-hydroxytamoxifen (TAM)]. As discussed, such acceptors are too large to pass through the pore that forms in response to nucleotide binding. When PAP is bound to SULT1A1, the isomerization equilibrium constant, K_{iso}, is 26 in favor of pore closure,[14] and large acceptors bind 26-fold more weakly to the nucleotide-bound form of the enzyme.[14] It should be noted that K_{iso} values obtained with PAP and PAPS are nearly identical.[13]

The affinities and stoichiometries of binding of TAM to SULT1A1 at 0 and 0.50 mM PAP (which is sufficient to saturate both nucleotide pockets) were determined by fluorescence titration (Figure 3A−C). The results, compiled in Table 2, reveal that the TAM affinities for E·PAP and E·(PAP)$_2$ are virtually identical (0.67 $\pm$ 0.08 and 0.65 $\pm$ 0.07 μM, respectively) and that each subunit of the dimer binds one acceptor. In contrast, when the PAP concentration favors the singly nucleotide-bound dimer, TAM binding is biphasic (Figure 4A,B). At 6.0 μM PAP, the distribution of forms is biased toward the E·PAP complex [E·PAP, 79%; E·(PAP)$_2$, 16%; E, 5.0%] and the affinities of the phases (0.67 $\pm$ 0.03 and 13 $\pm$ 2 μM) strongly suggest that the cap of one subunit is open while that of the other is closed. To confirm that each dimer contains a single high-affinity site, a "stoichiometry" titration was performed at a dimer concentration of 9.0 μM [i.e., 13$K_{d\ TAM}$, 24$K_{d\ PAP(high\ affinity)}$, and 0.3$K_{d\ PAP(low\ affinity)}$]. To maximize the concentration of singly bound species, the nucleotide concentration was set equal to that of the dimer, 9.0 μM. Under this condition, the distribution of forms is as
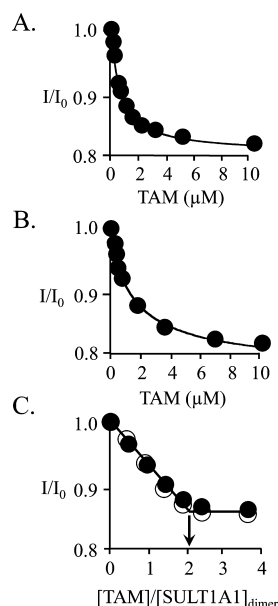
Figure 3. Binding of TAM to E and E·(PAP)$_2$. (A) TAM binding to E. Binding was monitored via changes in SULT1A1 intrinsic fluorescence (λ_{ex} = 290 nm; λ_{em} = 345 nm). Reaction conditions included SULT1A1 (0.10 μM, dimer), MgCl$_2$ (5.0 mM), NaPO$_4$ (50 mM), pH 7.2, and 25 ± 2 °C. Each point is the average of three independent determinations. The curve is the behavior predicted by a best fit model that assumes a single binding site per dimer. K_d = 0.67 ± 0.04. (B) TAM binding to E(PAP)$_2$. Conditions and data analysis were identical to those described for panel A except PAP = 0.50 mM (17K_d for PAPS binding at its low-affinity site). The K_d for TAM binding is 0.68 ± 0.12 μM. (C) Stoichiometry of binding of TAM to E and E·(PAP)$_2$. Conditions were identical to those described for panels A and B except that [SULT1A1] = 10 μM (dimer). Binding to E and E·(PAP)$_2$ is shown with filled and empty circles, respectively. The stoichiometries are 2.0 ± 0.1 TAM bound per SULT1A1 dimer.

Table 2. TAM and 1-HP Binding to SULT1A1

ligand	SULT1A1 species	K_d (μM)[a]
TAM	E	0.67 (0.08)
TAM	E·(PAP)$_2$	0.65 (0.07)
TAM	E·PAP	13 (2)
1-HP	E	8 (0.5)
1-HP	E·(PAP)$_2$	0.025 (0.001)
1-HP	E·PAP	0.025 (0.0010)

[a]Values in parentheses indicate one standard deviation.

follows: E·PAP, 77%; E·(PAP)$_2$, 3.8%; E, 19%. Both high- and low-affinity sites are observed in the titration, and the inset reveals that each dimer contains a single high-affinity TAM binding site.

Together, the nucleotide and TAM binding studies indicate that binding of the first nucleotide stabilizes the cap in the adjacent subunit in the open position, and in this configuration, only one acceptor site is open. When the second nucleotide binds, all nucleotide and acceptor sites open. What remains is to determine whether the open acceptor site in the singly occupied enzyme is located on the subunit to which PAPS is bound. This issue is addressed in the following section.

Linking to Reactivity. To assess whether PAPS occupancy influences SULT1A1 reactivity, the initial rate enzyme turnover was studied under conditions in which one or both of the dimer subunits were bound to nucleotide. The initial rate mechanism
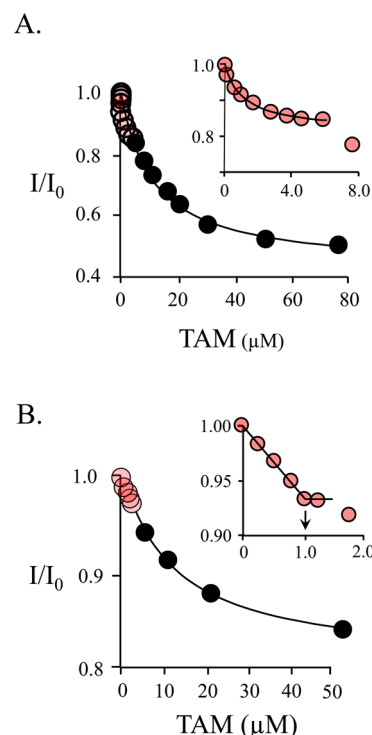

Figure 4. Binding of TAM to SULT1A1. (A) TAM binding is biphasic. Binding was monitored via changes in SULT1A1 intrinsic fluorescence (λ_{ex} = 290 nm; λ_{em} = 345 nm). The titration conditions included SULT1A1 (0.10 μM, dimer), PAP (6.0 μM), MgCl$_2$ (5.0 mM), NaPO$_4$ (50 mM), pH 7.2, and 25 ± 2 °C. The distribution of enzyme forms at 6.0 μM PAP is as follows: E·PAP, 79%; E·(PAP)$_2$, 16%; E, 5.0%. The first phase (red dots, inset) shows binding of TAM to the PAP-free subunit of SULT1A1 (K_d = 0.67 ± 0.05 μM). The second phase shows binding of TAM to the nucleotide-bound subunit (K_d = 13 ± 2 μM). Each point is the average of two independent determinations. The line through the points is the behavior predicted by a best-fit model that assumes a single binding site per dimer. The first and second phases were fit separately using the data indicated by the red and black circles, respectively. (B) Semiquantitative stoichiometric binding of TAM. The conditions of the titration included SULT1A1 (9.0 μM, dimer), PAP (9.0 μM), MgCl$_2$ (5.0 mM), NaPO$_4$ (50 mM), pH 7.2, and 25 ± 2 °C. At these concentrations, the distribution of enzyme forms is as follows: E·PAP, 77%; E·(PAP)$_2$, 3.8%; E, 19%. The binding is biphasic. The first phase (red dots, inset) indicates a stoichiometry of approximately one TAM binding site per dimer. A second low-affinity phase is also observed (black dots).

of SULT1A1 is sequential, rapid equilibrium random;[21] that is, a reactive ternary complex can form with either substrate binding first, and substrate binding reactions are near equilibrium during turnover.[12,21] In such mechanisms, steady-state affinity constants are excellent approximations of thermodynamic binding constants. Experiments were performed with small and large acceptors [1-hydroxypyrine (1-HP) and TAM]. [^{35}S]PAPS was used to monitor formation of sulfonated TAM (see Materials and Methods and Figure S2 of the Supporting Information). 1-HP and its sulfonated counterpart, 1-HPS, are fluorescent (Figure S3 of the Supporting Information). At the wavelengths used to monitor 1-HPS formation (λ_{ex} = 320 nm; λ_{em} = 380 nm), the fluorescence intensity of 1-HP is ~1% of that of 1-HPS. To establish experimental benchmarks for the 1-HP studies, the affinities of 1-HP for the three requisite forms of the enzyme [E, E·PAP,

and E·(PAP)$_2$] were determined by fluorescence titration (Figure S4A–C of the Supporting Information). The K_d values are compiled in Table 2 and reveal that, like other substrates,[22,23] 1-HP and nucleotide bind synergistically.

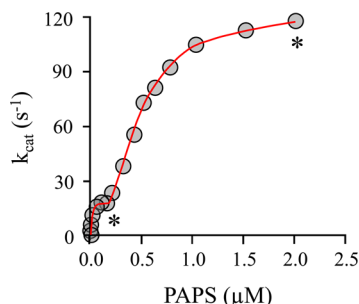When SULT1A1 turnover is plotted versus PAPS concentration at a saturating 1-HP concentration (Figure 5), distinct

Figure 5. SUTL1A1 turnover as a function of PAPS occupancy. A plot of SULT1A turnover vs [PAPS] is biphasic. The first and second phases correspond to saturation of the high- and low-affinity PAPS binding sites, respectively. The reaction was monitored via 1-HPS fluorescence (λ_{ex} = 320 nm; λ_{em} = 380 nm). The conditions included SULT1A1 (1.0 nM, dimer), 1-HP (160 μM, 20K_d), MgCl$_2$ (5.0 mM), NaPO$_4$ (50 mM), pH 7.2, and 25 ± 2.0 °C. The asterisks indicate the PAPS concentrations (0.20 and 2.0 μM) used in initial rate studies to obtain Michaelis parameters for the E·PAP and E·(PAPS)$_2$ forms.

low- and high-PAPS affinity phases are observed. To quantitate the differences in initial rate behavior of the singly and doubly occupied enzyme, initial rate experiments were performed at PAPS concentrations fixed in the plateau region of each phase (see asterisks in Figure 5). Table 3 lists the initial rate

Table 3. Initial Rate Parameters for E·PAP and E·(PAP)$_2$ Forms of SULT1A1

substrate	SULT1A1 species	K_m (μM)[a]	k_{cat} (s^{-1})[a]	[PAPS] (μM)
1-HP	E·PAP	0.041 (0.002)	130 (20)	0.30
1-HP	E·(PAP)$_2$	0.044 (0.03)	1000 (60)	2.0
TAM	E·PAP	14 (1.0)	2.0 (0.3)	4.0
TAM	E·(PAP)$_2$	0.60 (0.03)	11 (1.0)	250

[a]Values in parentheses indicate one standard deviation.

parameters associated with 1-HP sulfonation and the PAPS concentrations at which they were determined. As expected for a small acceptor, K_m for 1-HP is not affected by PAPS occupancy; however, k_{cat} increases nearly 8-fold. If the increased rate of turnover were due solely to PAPS saturation at the second site, a 2-fold increase would have occurred. Thus, as the caps are opened at both sites, each subunit turns over 4 times more quickly than the subunit in the singly occupied enzyme.

Equilibrium binding constants (Table 2) were used to select the PAPS concentrations, 4.0 and 250 μM, used in the TAM initial rate studies. At 4.0 μM PAPS, the majority of SULT1A1 has a single nucleotide bound [E·PAP, 82%; E·(PAP)$_2$, 1.1%; E, 10%]. At 250 μM PAPS, the enzyme is primarily in the doubly occupied form [E·(PAP)$_2$, 89%; E·PAP, 10%; E, <0.1%]. The results are listed in Table 3. The fact that the TAM K_m values are nearly identical to their corresponding K_d values (Table 2) confirms that binding is near equilibrium during turnover. On the basis of the TAM equilibrium binding studies, it was not possible to determine whether, for the singly occupied enzyme,

the high-affinity TAM binding site is situated on the subunit that is bound to PAPS. If the high-affinity site were located on the PAPS-bound subunit, the K_m would equal the high-affinity K_d; if not, it would equal the low-affinity K_d. The TAM K_m value, 14 μM, is nearly equal to the K_d for the low-affinity site, 13 μM; hence, the high-affinity binding site is located on the empty subunit of the singly occupied enzyme. The ratio of the TAM K_m for the singly and doubly occupied enzyme is 23. This value is nearly equal to the cap isomerization equilibrium constant, 26,[14] and indicates that the cap has gone from largely closed to largely opened as the second nucleotide binds, a finding that is completely consistent with the TAM equilibrium binding data.

The results of the initial rate studies clearly indicate that the allosteric interactions that govern nucleotide binding also regulate the reactivity of the enzyme. For small substrates, the effects are primarily on k_{cat}, and the catalytic efficiency (V/K) of the enzyme increases by a factor of ~8. For large substrates, both k_{cat} and K_m are affected, with the result that the efficiency for such substrates increases 130-fold as the system moves from the singly to doubly occupied state. These two states represent end points on a sliding scale of catalytic efficiency whose set point is determined by the nucleotide concentration.

A Biological Raison d'Etre. For the PAPS concentration to be used to regulate SULT1A1 reactivity in the cell, its *in vivo* concentration must be sufficiently high to populate the second nucleotide binding site. PAPS levels have been quantitated in numerous human tissues that express SULT1A1,[24−27] and its concentrations can be calculated using tissue-specific, weight/volume conversion factors.[28] While these calculations are gross in that they assume a uniform distribution of nucleotide throughout the tissue, they nevertheless provide a likely lower limit of the cellular PAPS concentration. These concentrations were used to calculate the fraction of dimers that have PAPS bound at both subunits in the various tissues (Figure 6). The
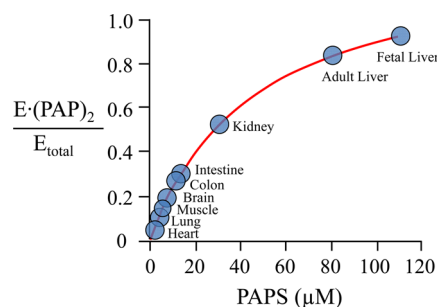

Figure 6. Predicted fraction of E·(PAPS)$_2$ in human tissues. Fractions were calculated using reported PAPS concentrations.[24−27]

calculations predict that PAPS concentrations in all tissues are sufficiently high to saturate the first subunit, but only in certain tissues is it high enough to substantially populate the second.

As SULT1A1 becomes doubly occupied, k_{cat} increases 8-fold; the catalytic capacity of the system increases by a factor of nearly 10, and K_m decreases ~25-fold for only large substrates. This selective bias places large and small substrates on a catalytic "par"; their k_{cat}/K_m values become comparable at double occupancy. One of the important functions of SULT1A1 is to detoxify xenobiotics as they pass through the liver. While this enormous class of compounds is far from fully characterized, many can be classified as large substrates. Thus, in tissues in which the defensive role of SULT1A1 is

particularly important, the enzyme seems likely to operate in the double-occupancy mode, which is precisely what the calculations predict. In liver, where the defensive function is arguably the most important of any organ, the enzyme is predicted to be almost entirely in the double-occupancy state. In organs like kidney and intestine, where the demand for defensive function is weaker, but still significant, the curve predicts that the enzyme is balanced between single- and double-occupancy states and is thus poised to respond to PAPS concentration and xenobiotic "load". Finally, in tissues like heart and brain, where the load is presumably slight, the enzyme is nearly exclusively in its low-efficiency state. In summary, it appears that PAPS concentrations *in vivo* are indeed sufficiently high to regulate SULT1A1 reactivity, and remarkably, the enzyme's performance with respect to turnover and substrate specificity will be highly tissue dependent.

CONCLUSIONS

PAPS binds antisynergistically to the subunits of the SULT1A1 dimer. Nucleotide binding at the first subunit causes an 81-fold weakening in the affinity at the second. The decreased affinity is due solely to an increase in the nucleotide off rate constant, which strongly suggests that the cap at the weak affinity site is stabilized in the open position. To determine the cap configurations at all four ligand binding sites as a function of PAPS occupancy, cap positioning at the acceptor pockets was determined using large and small acceptors. PAPS binding at the first site closes both the nucleotide and acceptor cap segments only on the subunit to which PAPS is bound; the cap on the adjacent subunit remains open at both sites. Once the second nucleotide adds, the caps open at all four ligand binding pockets. The coupling of PAPS binding and cap closure is depicted in Figure 7. In this configuration, k_{cat} is increased 8-fold relative to that of the singly PAPS-bound enzyme, and K_m decreases 23-fold toward large substrates. Finally, estimates of PAPS concentrations across a variety of tissues suggest that SULT1A1 reactivity will be highly tissue-dependent, and that the enzyme will function in its broadest specificity and highest
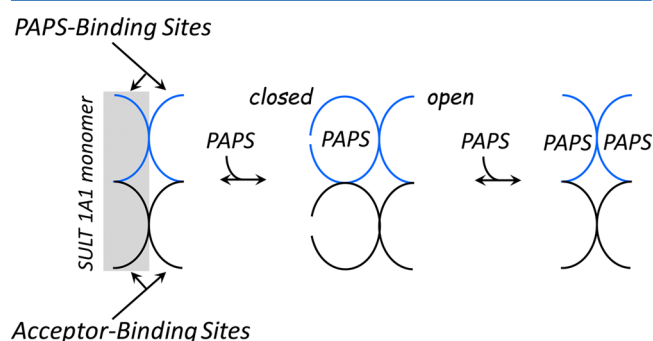

Figure 7. Coupling of PAPS binding and cap closure in SULT1A1. The ligand binding sites of the unliganded enzyme are open and can receive ligands. Binding of the first PAPS molecule closes both the PAPS and acceptor binding sites of the subunit to which PAPS has bound. In this configuration, PAPS cannot escape and only small acceptors can enter unless the enzyme isomerizes to the open form (not shown), which is unfavorable (K_{iso} = 26 in favor of the closed state). Consequently, the singly PAPS-bound configuration favors small acceptors. As the second PAPS molecule binds, all of the binding sites open, thus alleviating the catalytic bias against large substrates, and each subunit turns over 4-fold faster.

turnover mode in tissues that experience the highest levels of xenobiotics.

ASSOCIATED CONTENT

Ⓢ Supporting Information

Pre-steady-state binding of PAPS to SULT1A1 (Figure S1), TAM initial rate studies (Figure S2), fluorescence spectra of 1-HP and 1-HPS (Figure S3), and 1-HP binding to the E and E·(PAP)₂ forms of SULT1A1 (Figure S4). This material is available free of charge via the Internet at http://pubs.acs.org.

AUTHOR INFORMATION

Corresponding Author

*Department Microbiology and Immunology, Albert Einstein College of Medicine, 1300 Morris Park Ave., Bronx, NY 10461-1926. E-mail: tom.leyh@einstein.yu.edu. Phone: (718) 430-2857. Fax: (718) 430-8711.

Notes

The authors declare no competing financial interest.

ABBREVIATIONS

HEPES, *N*-(2-hydroxyethyl)piperazine-*N*′-2-ethanesulfonic acid; MBP, maltose binding protein; PAP, 3′,5′-diphosphoadenosine.

REFERENCES

(1) Falany, J. L., Macrina, N., and Falany, C. N. (2002) Regulation of MCF-7 breast cancer cell growth by *β*-estradiol sulfation. *Breast Cancer Res. Treat.* 74, 167−176.

(2) Falany, J. L., and Falany, C. N. (1996) Regulation of estrogen sulfotransferase in human endometrial adenocarcinoma cells by progesterone. *Endocrinology* 137, 1395−1401.

(3) Steventon, G. B., Heafield, M. T., Waring, R. H., and Williams, A. C. (1989) Xenobiotic metabolism in Parkinson's disease. *Neurology* 39, 883−887.

(4) Li, L., and Falany, C. N. (2007) Elevated hepatic SULT1E1 activity in mouse models of cystic fibrosis alters the regulation of estrogen responsive proteins. *J. Cystic Fibrosis* 6, 23−30.

(5) Moore, K. L. (2003) The biology and enzymology of protein tyrosine O-sulfation. *J. Biol. Chem.* 278, 24243−24246.

(6) Nowell, S., and Falany, C. N. (2006) Pharmacogenetics of human cytosolic sulfotransferases. *Oncogene* 25, 1673−1678.

(7) Leyh, T. S. (1993) The physical biochemistry and molecular genetics of sulfate activation. *Crit. Rev. Biochem. Mol. Biol.* 28, 515−542.

(8) Falany, C. N. (1997) Enzymology of human cytosolic sulfotransferases. *FASEB J.* 11, 206−216.

(9) Visser, T. J. (1994) Role of sulfation in thyroid hormone metabolism. *Chem.-Biol. Interact.* 92, 293−303.

(10) Robertson, J. F., and Harrison, M. (2004) Fulvestrant: Pharmacokinetics and pharmacology. *Br. J. Cancer* 90 (Suppl. 1), S7−S10.

(11) Riches, Z., Stanley, E. L., Bloomer, J. C., and Coughtrie, M. W. (2009) Quantitative evaluation of the expression and activity of five major sulfotransferases (SULTs) in human tissues: The SULT "pie". *Drug Metab. Dispos.* 37, 2255−2261.

(12) Cook, I., Wang, T., Falany, C. N., and Leyh, T. S. (2012) A Nucleotide-Gated Molecular Pore Selects Sulfotransferase Substrates. *Biochemistry* 51, 5674−5683.

(13) Leyh, T. S., Cook, I., and Wang, T. (2013) Structure, dynamics and selectivity in the sulfotransferase family. *Drug Metab. Rev.* 45, 423−430.

(14) Cook, I., Wang, T., Almo, S. C., Kim, J., Falany, C. N., and Leyh, T. S. (2013) The gate that governs sulfotransferase selectivity. *Biochemistry 52*, 415−424.

(15) Cook, I., Wang, T., Falany, C. N., and Leyh, T. S. (2013) High Accuracy In-Silico Sulfotransferase Models. *J. Biol. Chem. 288*, 34494−34501.

(16) Zhang, H., Varlamova, O., Vargas, F. M., Falany, C. N., and Leyh, T. S. (1998) Sulfuryl transfer: The catalytic mechanism of human estrogen sulfotransferase. *J. Biol. Chem. 273*, 10888−10892.

(17) Sun, M., and Leyh, T. S. (2010) The human estrogen sulfotransferase: A half-site reactive enzyme. *Biochemistry 49*, 4779−4785.

(18) Johnson, K. (1992) Transient-state kinetic analysis of enzyme reaction pathways. In *The Enzymes* (Sigman, D. S., Ed.) pp 1−61, Academic Press, New York.

(19) Cleland, W. W. (1979) Statistical analysis of enzyme kinetic data. *Methods Enzymol. 63*, 103−138.

(20) Cook, I., Wang, T., Almo, S. C., Kim, J., Falany, C. N., and Leyh, T. S. (2013) Testing the Sulfotransferase Molecular Pore Hypothesis. *J. Biol. Chem. 288*, 8619−8626.

(21) Wang, T., Cook, I., Falany, C. N., and Leyh, T. S. (2014) Paradigms of Sulfotransferase Catalysis: The Mechanism of SULT2A1. *J. Biol. Chem. 289*, 26474−26480.

(22) Tyapochkin, E., Cook, P. F., and Chen, G. (2008) Isotope exchange at equilibrium indicates a steady state ordered kinetic mechanism for human sulfotransferase. *Biochemistry 47*, 11894−11899.

(23) Whittemore, R. M., Pearce, L. B., and Roth, J. A. (1986) Purification and kinetic characterization of a phenol-sulfating form of phenol sulfotransferase from human brain. *Arch. Biochem. Biophys. 249*, 464−471.

(24) Brzeznicka, E. A., Hazelton, G. A., and Klaassen, C. D. (1987) Comparison of adenosine 3′-phosphate 5′-phosphosulfate concentrations in tissues from different laboratory animals. *Drug Metab. Dispos. 15*, 133−135.

(25) Cappiello, M., Franchi, M., Giuliani, L., and Pacifici, G. M. (1989) Distribution of 2-naphthol sulphotransferase and its endogenous substrate adenosine 3′-phosphate 5′-phosphosulphate in human tissues. *Eur. J. Clin. Pharmacol. 37*, 317−320.

(26) Pacifici, G. M., Franchi, M., Colizzi, C., Giuliani, L., and Rane, A. (1988) Sulfotransferase in humans: Development and tissue distribution. *Pharmacology 36*, 411−419.

(27) Sakakibara, Y., Yanagisawa, K., Katafuchi, J., Ringer, D. P., Takami, Y., Nakayama, T., Suiko, M., and Liu, M. C. (1998) Molecular cloning, expression, and characterization of novel human SULT1C sulfotransferases that catalyze the sulfonation of N-hydroxy-2-acetylaminofluorene. *J. Biol. Chem. 273*, 33929−33935.

(28) McIntosh, R. L., and Anderson, V. (2010) A Comprehensive Tissue Properties Database Provided for the Thermal Assessment of a Human at Rest. *Biophys. Rev. Lett. 5*, 129.